

Feature Extraction and Analysis using Gabor Filter and Higher Order Statistics for the JPEG Steganography

SwagotaBera¹, Dr. Monisha Sharma² and Dr. Bikesh Singh³

¹*Department of Electronics & Telecommunication Engineers
Shri Shankaracharya College of Engineering and Technology-SSCET, Bhilai,
Chhattisgarh 491001, India.*

²*Department of Electronics & Telecommunication Engineers,
Shri Shankaracharya College of Engineering and Technology-SSCET, Bhilai,
Chhattisgarh 491001, India.*

³*Department of Bio-Medical Engineering, National Institute of Technology- NIT, Raipur,
Chhattisgarh 492001, India.*

Abstract

Objective: In the proposed work the efficiency of JPEG steganalysis is tried to increase with the implementation of higher order statistics.

Methods/Statistical analysis: After embedding the secret data in an image causes deviations in the texture and characteristics in image which can be captured through the Gabor filter of two dimension for the different orientations and scales. The higher order statistical attributes are obtained which generates the image features and then PCA (Principal Component analysis) is implemented for the feature selection and reduction of the image features dimension which finally generates GFB (Gabor Filter Based) image feature. GFB are extracted for the images in database and then random forest based data mining is implemented for the performance analysis. GFB is implemented to detect the present state of art steganography JUNIWARD and nsF5 for the different payload 0.05, 0.1 and 0.2 bpac (bits per non-zero a.c. coefficient).

Findings: On comparing the detection accuracy and the execution time of the presented method with the existing JPEG steganalysis i.e. DCTR (Discrete Cosine Transform Residual) and GFR (Gabor Filter Residual) it is the finding that the execution time gets reduced and shows better detection accuracy.

Application/Improvements: It is having wide applications in smart id generation, forgery detection in forensic department and also to suspect the terrorist activities. Increase in the detection efficiency will be helpful to have prior information about any antisocial act.

Keywords: Steganography, Steganalysis, DCT, SVM, WEKA, Gabor filter

INTRODUCTION

Image steganography is the art of concealing data in an image and in contrary steganalysis is detection of concealed data in

an image. Since 1998 to till date the research in JPEG steganography and steganalysis techniques made rigorous progress in the research field. In the journey of the steganalysis research the researchers tried to develop more and more complex hiding process so that it can be less detectable. So it becomes the requirement to embellish the steganalysis methodology for increasing the detection capability. The complexity of the hiding technique gets increased in the introduction of the content adaptive steganography which makes more difficult to design detection technique. In the non-adaptive steganography i.e. in Jsteg [1], Outguess [2], F5 [3], nsF5 [4], MB (Model Based) [5] and PQ (Perturbed Quantization) [6] are few techniques developed and later the content adaptive hiding techniques such as Texture Adaptive PQ is abbreviated as PQt [7], Model Optimized Distortion is abbreviated as MOD [8], Uniform Embedding Distortion is abbreviated as UED [9], JPEG UNiversal Wavelet Relative Distortion is abbreviated as JUNIWARD [10] are being developed. In all the content adaptive steganography the distortion function is first find out and then messages are concealed with minimum distortion which increases the steganography security. The different content adaptive steganographic technique used different distortion function which depends on the texture and energy content of the image. The content adaptive steganography is more secure than non-adaptive steganography. In this paper, our concentration is on the steganalysis for the content adaptive steganography.

In the history of universal steganalysis, the trend is to extract the image features which get transformed after information hiding because their existing correlation. The features can be obtained either from the spatial domain or in the domain where image gray level values are transformed to other values by implementing any specific transformation mathematics. Almost in all the image steganalysis it is tried to find out the image statistical features that represents the statistical variations of the image coefficients. These statistical features are extracted from various pre-processed images. Various pre-processing used are finding of DCT (Discrete Cosine

Transformation) [11], DWT (Discrete Wavelet Transformation) [12], Image Segment and Calibration [13], Intra and Inter Block Difference Block from spatial and transform domain [14] and STFT (Short Time Fourier Transform) [15, 16] or Gabor Transform.

The different statistical features in the transform domain are mathematical statistics of wavelet coefficients [17], higher order statistics of DCT coefficients with the calibration concept [18], Markov's features [19], Merged DCT and Markov's features named as CCPEV (Cartesian Calibrated Features) [20]. In almost all the cases the feature dimension goes on increasing and the target is to increase the detection accuracy. In the recent trend in the steganalysis designing, the concentration is more towards the designing of the projection model which is constrained to the complex texture region of the image which mainly target to detect the content adaptive steganography. The CC-JRM (Cartesian Calibrated JPEG Rich Model) is based on the intra and inter-block co-occurrence [21] is one of them. There came a great change in the steganalysis designing with the introduction of DCTR (Discrete Cosine Transform Residual [22] technique. In DCTR feature, the convolution of the uncompressed JPEG image is done with each 64 kernels of the DCT and then by subsampling the residual images the histogram of the quantized noise residuals are obtained. This technique provides better detection accuracy that the previous techniques. Again a better technique was introduced i.e. PHARM (Phase-Aware Projection Model) [23], which utilizes the pixel residuals of JPEG images and their phase for an 8×8 grid. A 2D Gabor filter was introduced for finding the texture of image characteristics obtained from various scales and orientations and then first and higher order statistical features are obtained in GFR [15] and GRF (Gabor Rich Filter) [24]. Since introduction of Gabor filter increases the detection accuracy of the content adaptive steganography such as J-UNIWARD. The accuracy of the JUNIWARD which is content-adaptive JPEG steganographic schemes is more accurate. Deploying of the Gabor filter in the steganalysis verified to be a better tool for the scheming of the image steganalysis.

The acquired statistical features from the stego and non-stego images are deployed for the training and the testing of the adopted classifier so that it developed to be software based empirical machine for the perception of any secret messages in an unknown media image. Various well known feasible classifiers are FLD (Fischer Linear Discriminator) [22], SVM (Support Vector Machine) [25], Ensemble Classifier [24], CNN (Convolutional Neural Network) [13] and Random Forest [12] as suggested in the popular research papers. The surveillance of referred research paper deduces that the feature dimensions goes on increasing with the introduction of improved steganalysis technique. Although increasing feature set increases the detection accuracy but increases the execution time and the memory cost. So, proper feature selection and reduction skill technique can be is introduced which reduces the feature dimension without affecting the detection accuracy. Few of them suggested in the cited research papers are Markov Random Field (MRF) Cliques [25], ITERATIVE BEST Strategy [21], Improved Firefly

Algorithm-DyFA and Fitness function –SVM [11], ANOVA (Analysis of Variance) [12], ABC (Artificial Bee Colony) [29] and on the basis of highest detection accuracy [24].

In this paper, an GFB is introduced in which feature extraction and selection is employed using higher order statistical parameters of the GFB (Gabor Filter Based) steganalysis [15]. The 2D Gabor transform is deployed to be a pre-processing tool. The Gabor filtering is done on the decompressed JPEG images for sketching the image texture characteristics and then first order statistical parameter histogram is calculated. The feature dimension depends on the values of the preferred parametric values for the Gabor filter generation. The final image features are acquired on merging the raw histogram features. Then PCA is employed for the feature selection and reduction of final image features and GFB is obtained with ample reduced dimension. The dimension value is decided on the fact that reduced dimension must not affect the detection accuracy.

In section 2, the 2-D Gabor filter and its properties is discussed. In section 3, the feature obtaining technique is introduced. In section 4, PCA feature selection is implemented and the detection performance is evaluated. In section 5, the conclusion is drawn and discussed.

GABOR FILTERING

Gabor filter of Two Dimension

Gabor filter is the implementation of the Gabor transform which is a short term Fourier transformation with Gaussian window for analysis in the spatial domain. The distortion information of content adaptive image steganography incorporates the texture information of the image. On embedding there causes texture anomaly in an image. This texture anomaly can be characterized by the Gabor output obtained by 2D Gabor filtering. The two dimensional Gabor filter represents the texture information because of its spatial selectivity and orientation [24].

For obtaining the Gabor residuals $u(x, y)$, convolution of an image $I(x, y)$ is done with a two dimensional Gabor function $g(x, y)$ as represented in equation (1) and in equation (2).

$$u(x, y) = \iint_{\delta} I(\alpha, \beta) g(x - \alpha, y - \beta) d\alpha d\beta \quad (1)$$

Where, the set of image points are $(x, y) \in \delta$, δ and the integral variables are α and β .

$g(x, y)$ is the Gabor function

$$g_{\lambda, \theta, \varphi, \sigma, \gamma}(x, y) = \exp\left(-\frac{(x^2 + \gamma^2 y^2)}{2\sigma^2}\right) \cos\left(2\pi \frac{x}{\lambda} + \varphi\right) \quad (2)$$

Where

$$x = a \cos \theta + b \sin \theta$$

$$y = -a \sin \theta + b \cos \theta$$

λ -- Wavelength of Gabor function cosine factor.
 θ -- Orientation of Gabor function normal to the parallel stripes.
 φ -- Phase offset of the of Gabor function cosine factor.
 σ -- Standard deviation sigma of Gaussians function.
 γ -- Ellipticity of the Gaussian factor.

The small value of σ specifies high spatial resolution and high value specifies a low spatial resolution. The value of σ determines window size of the Gaussians function. The values of the parameter θ are real values which belongs in the range from 0 and π , and parameter φ decides the symmetry of the Gabor filter: if $\varphi = 0, \pi$, the filter is Centro symmetric, and if $\varphi = -\pi/2, \pi/2$, he filter is anti-Centro symmetric. The Gabor mean is set to zero. In the frequency domain only two peaks are observed for the cosine term which is multiplied with the frequency term of the Gaussian function. Scale parameter and orientation parameter value is decided by the detection accuracy value of the corresponding features.

The 2D Gabor filter can be discretized in the order M x N by setting the ranges of x and y. Then the 2D Gabor filter is generated according to the value set for the parameters. In the paper, the order of M x N is 8 x 8.

In figure (1), 2D Gabor filter is shown with different orientations and phase offset. In figure (1a), the filter is centrosymmetric and anti-centrosymmetric in figure (1b). Different filters can be generated depending on the different values of the orientation parameters.

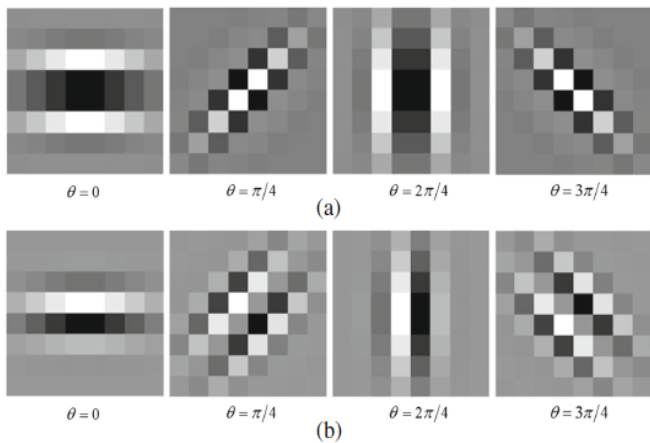


Figure 1. 2D Gabor filters for $\sigma = 1$ (a) $\varphi = 0$ (Centrosymmetric) (b) $\varphi = \pi/2$ (Anti-centrosymmetric)

In figure (2), the Gabor filter is represented for different orientations, phase offset and deviations. The two highlighted circle in the frequency domain is due to the two peak values of the cosine term and the separation of the two peaks are decided by the phase offset and the number of spatial domain values also get varied.

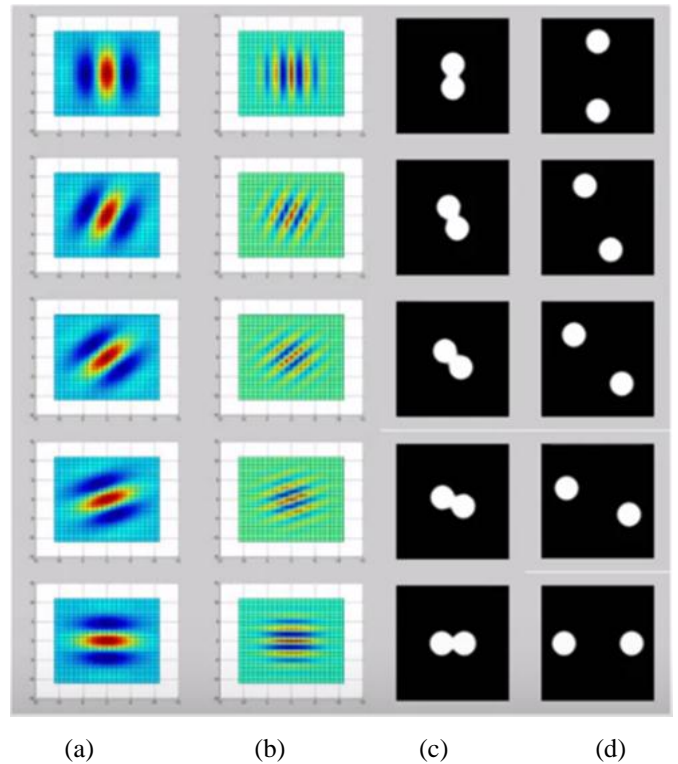


Figure 2. Representation of Gabor filter for orientation values of 0, 22.5, 45, 67.5 and 90 for (a) Low offset spatial domain (b) High offset spatial domain (c) Low offset frequency domain (d) High offset frequency domain

In figure (3), Gabor residual image is shown for different standard deviation value for different orientations and phase offset of $\pi/2$ implemented on the Leena image. In figure (3a), σ value is low and so the textures and edges of the image are apparent as compared when σ value is high in figure (3b). Different filters can be generated depending on the different values of the orientation parameters.

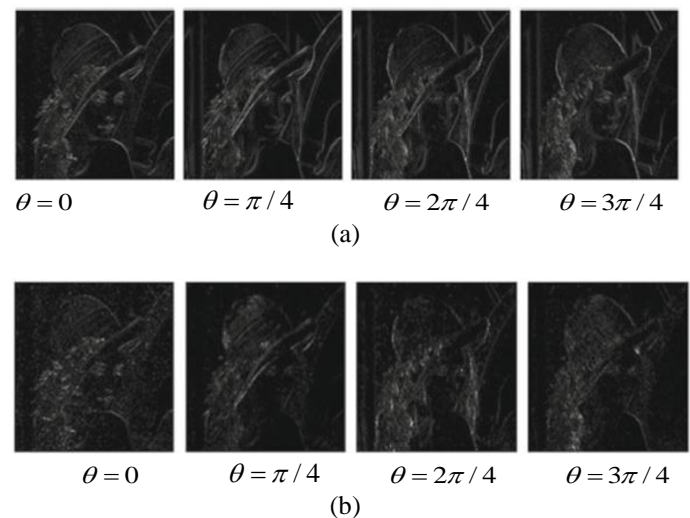


Figure 3. Gabor residual for $\varphi = \pi/2$ (a) $\sigma = 0.5$ (High spatial resolution) (b) $\sigma = 1$ (Low spatial resolution)

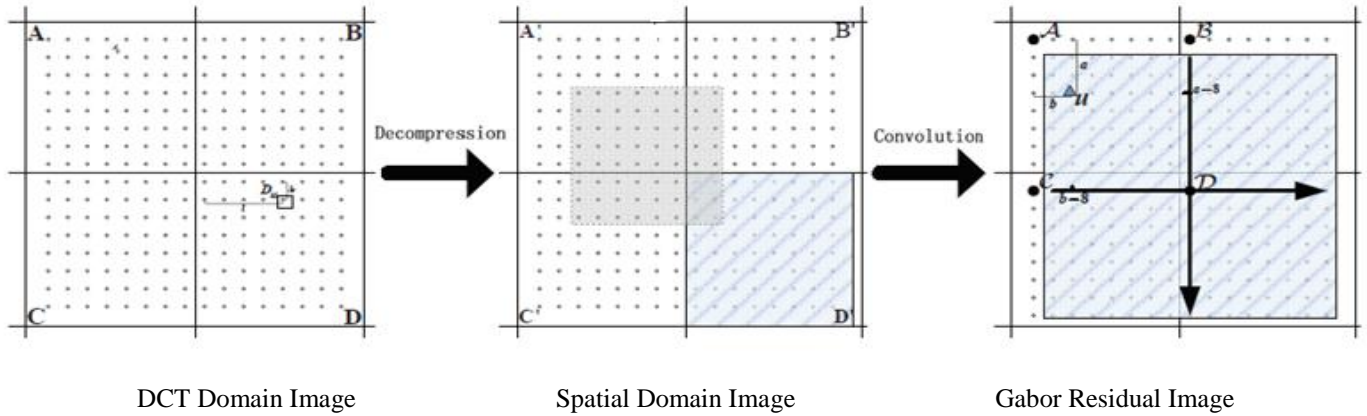


Figure 4. Representation of the effects of Gabor filter on the image

Properties of Gabor residuals

The JPEG image is first decompressed and then filtered image is obtained $U^{(s,l)} = I * G^{(s,l)}$, where $G^{(s,l)}$ represents Gabor filter of two dimensions having s scale and l orientation and I is decompressed image.

In figure (4), it is shown that a change of one DCT coefficient in DCT domain affects 8×8 neighbourhood pixels in D whereas modifies 15×15 neighbourhood pixels in the Gabor residuals which is represented in equation (3)

$$R^{(s,l)}(i,j) = G^{(s,l)} \otimes B(i,j) \tag{3}$$

Where (i,j) depicts the DCT mode, $R^{(s,l)}(i,j)$ depicts the DCT coefficient, $G^{(s,l)}$ represents

Gabor filters and \otimes represents the cross-correlation. In figure (4), the value $u \in U^{(s,l)}$ in Gabor residual and can be evaluated as in equation (4).

$$u = \sum_{i=0}^7 \sum_{j=0}^7 Q_{i,j} \begin{bmatrix} A_{i,j} R_{a,b}^{(\varphi,\sigma,\theta)}(i,j) + B_{i,j} R_{a,b-8}^{(\varphi,\sigma,\theta)}(i,j) \\ + C_{i,j} R_{a-8,b}^{(\varphi,\sigma,\theta)}(i,j) + D_{i,j} R_{a-8,b-8}^{(\varphi,\sigma,\theta)}(i,j) \end{bmatrix} \tag{4}$$

For a and b is from 0 to 7. The value u can be represented by projection vector $P_{a,b}^{(s,l)}(i,j)$ as in equation (5):

$$u = \begin{pmatrix} Q_{00} A_{00} \\ \vdots \\ Q_{00} A_{00} \\ Q_{00} A_{00} \\ \vdots \\ Q_{00} A_{00} \\ Q_{00} A_{00} \\ \vdots \\ Q_{00} A_{00} \\ Q_{00} A_{00} \\ \vdots \\ Q_{00} A_{00} \\ Q_{00} A_{00} \\ \vdots \\ Q_{00} A_{00} \end{pmatrix}^T \begin{pmatrix} R_{a,b}^{(s,l)}(1,1) \\ \vdots \\ R_{a,b}^{(s,l)}(8,8) \\ R_{a,b-8}^{(s,l)}(1,1) \\ \vdots \\ R_{a,b-8}^{(s,l)}(1,1) \\ R_{a-8,b}^{(s,l)}(1,1) \\ \vdots \\ R_{a-8,b}^{(s,l)}(1,1) \\ R_{a,b}^{(s,l)}(1,1) \\ \vdots \\ R_{a-8,b-8}^{(s,l)}(1,1) \end{pmatrix} \tag{5}$$

Where $R_{a,b}^{(s,l)}(i,j)$ is unit response which is centrosymmetric.

FEATURE EXTRACTIONS

The two dimensional Gabor filter is generated in which s denoted the different s values of the standard deviation and l represents the orientation numbers for each scale. For a particular value of s and l the number of Gabor filters is $2.s.l$. The higher order statistical parameters are obtained from the filtered image coefficients $U^{s,l}$ which are known as image features. The global histogram, local histogram, variations, blockiness, co-occurrence matrices, dual histogram and Markov features are calculated covers the inter-block and intra-block dependencies.

Image Features

The statistical parameters are evaluated from the filtered images are known as image features.

Global Histogram

Suppose, $d_{ij}(k)$ represents (i,j)-th gabor filter coefficient in subsamples for the k-th block. The first functional is the global histogram of all 64 subsamples of all the image blocks in equation (6). H represents the global histogram.

$$H = (H_L, \dots, H_R) \tag{6}$$

Where $L = \min_{i,j,k} d_{i,j}(k)$

$$R = \max_{i,j,k} d_{i,j}(k)$$

Most of steganographic programs preserve global histogram whereas fails to restore the histogram of the individual modes. For a particular mode (i, j), let h_r^{ij} , $r = L, \dots, R$, denote the individual histogram of values $d_k(i, j)$.

Local Histogram

These functionals are the local histogram for the five modes $(i, j) \in \{(1, 2), (2, 1), (3, 1), (2, 2), (1, 3)\}$ calculated using equation (7).

$$h^{ij} = (h_L^{ij}, \dots, h_R^{ij}) \tag{7}$$

Dual Histogram

The dual histogram is calculated using equation (8) where the number of times value d occurs as (i, j)-th coefficient in the image subsample is represented by g_{ij}^d .

$$g_{ij}^d = \sum_{(k=1)}^{n_B} \delta(d, d_{ij}(k)) \tag{8}$$

In the equation (5), $\delta(u,v)=1$ if $u=v$

$$\delta(u,v)=0 \text{ and } d= -5 \text{ to } +5[20].$$

Variations

The statistical parameters variations which captured the inter-block dependencies get violated by various steganographic algorithms. The vectors of block indices are I_r and I_c obtained through scanning the image by rows and columns, respectively for all the subsamples. In equation (6), the first functional is the variation V which captures the inter-block de-pendency.

$$V = \frac{\sum_{i,j=1}^8 \sum_{k=1}^{|I_r|-1} |d_{I_r(k)}(i,j) - d_{I_r(k+1)}(i,j)| + \sum_{i,j=1}^8 \sum_{k=1}^{|I_c|-1} |d_{I_c(k)}(i,j) - d_{I_c(k+1)}(i,j)|}{|I_r| + |I_c|}$$

Due to embedding changes the discontinuities along the 8x8 block boundaries get increases.

Blockiness

The blockiness measures B_α , $\alpha = 1, 2$, are calculated using equation (9). From the image subsamples, the blockiness parameters are calculated.

$$B_\alpha = \frac{\sum_{i=1}^{[(M-1)/8]} \sum_{j=1}^N |x_{8i,j} - x_{8i+1,j}|^\alpha + \sum_{j=1}^{[(N-1)/8]} \sum_{i=1}^M |x_{i,8j} - x_{i,8j+1}|^\alpha}{N[(M-1)/8] + M[(N-1)/8]} \tag{9}$$

In the equation (7), the image dimensions are M and N and x_{ij} are grayscale values.

Co-occurrence Matrices

From co-occurrence matrix of neighboring coefficients statistical parameter is calculated. For the given range $L \leq d_k(i, j) \leq R$, co-occurrence matrix C is a square $D \times D$ matrix, defined as in equation (10), has sharp peak at (0,0) and then falls off. The value $D = R - L + 1$.

$$C_{st} = \frac{\sum_{k=1}^{|I_r|-1} \sum_{i,j=1}^8 \delta(s, d_{I_r(k)}(i,j)) \delta(t, d_{I_r(k+1)}(i,j)) + \sum_{k=1}^{|I_c|-1} \sum_{i,j=1}^8 \delta(s, d_{I_c(k)}(i,j)) \delta(t, d_{I_c(k+1)}(i,j))}{|I_r| + |I_c|} \tag{10}$$

The strongly positively correlation in the image is for the values $(s, t) \in \{(0, 1), (1, 0), (-1, 0), (0, -1)\}$ and also $(s, t) \in \{(1, 1), (-1, 1), (1, -1), (-1, -1)\}$ [20].

Markov Features

The smoothness, continuity, regularity and periodicity of original image get deviates due to data hiding. The deviations caused due to the data hiding will be more exaggerated if the differences of the neighbouring elements in the block image coefficients are find out. For this purpose, four difference neighbouring matrices are considered which is evaluated from all image subsamples. These four difference neighbouring matrices are generated in the four directions i.e. horizontal, vertical, major diagonal and minor diagonal using equation (11).

$$\begin{aligned} F_h(u, v) &= F(u, v) - F(u + 1, v) \\ F_v(u, v) &= F(u, v) - F(u, v + 1) \\ F_d(u, v) &= F(u, v) - F(u + 1, v + 1) \\ F_m(u, v) &= F(u + 1, v) - F(u, v + 1) \end{aligned} \tag{11}$$

Where $u, v \in (m, n)$ where m and n value is the row and the column number of the image block. The horizontal, major diagonal, vertical and minor diagonal difference matrices are $F_h(u,v)$, $F_v(u,v)$, $F_d(u,v)$, and $F_m(u,v)$, respectively. The calculation of the differences of the pixels is within the same block. The values of the difference neighbouring arrays are restricted in the range of -4 to +4 value. The markov's transition probability matrix for all four difference

neighbouring arrays is used for obtaining the image features using equation (12).

$$M_h(i, j) = \frac{\sum_{u=1}^{S_u-2} \sum_{v=1}^{S_v} \delta(F_h(u, v) = i, F_h(u+1, v) = j)}{\sum_{u=1}^{S_u-1} \sum_{v=1}^{S_v} \delta(F_h(u, v) = i)}$$

$$M_v(i, j) = \frac{\sum_{u=1}^{S_u} \sum_{v=1}^{S_v-2} \delta(F_v(u, v) = i, F_v(u, v+1) = j)}{\sum_{u=1}^{S_u} \sum_{v=1}^{S_v-1} \delta(F_v(u, v) = i)}$$

$$M_d(i, j) = \frac{\sum_{u=1}^{S_u-2} \sum_{v=1}^{S_v-2} \delta(F_d(u, v) = i, F_d(u+1, v+1) = j)}{\sum_{u=1}^{S_u-1} \sum_{v=1}^{S_v-1} \delta(F_d(u, v) = i)}$$

$$M_m(i, j) = \frac{\sum_{u=1}^{S_u-2} \sum_{v=1}^{S_v-2} \delta(F_m(u+1, v) = i, F_m(u, v+1) = j)}{\sum_{u=1}^{S_u-1} \sum_{v=1}^{S_v-1} \delta(F_m(u, v) = i)} \quad (12)$$

Where $i, j \in \{-4, -3, -2, -1, 0, 1, 2, 3, 4\}$ and S_u and S_v represent the dimensions of image. The value $\delta = 1$ if and only if its argument are satisfied and zero otherwise. To decrease feature dimension, the average value is considered as the final feature dimension using equation (13) [20].

$$TPM = \frac{M_h + M_v + M_d + M_m}{4} \quad (13)$$

GFB Features

The proposed GFB feature extraction scheme has been depicted in figure (5) and consecutive steps are described briefly as follows:

Step 1: First of all the compression of input JPEG image I is performed for obtaining the image in spatial domain by skipping quantization such that there will be no loss of information.

Step 2: The value of scale (standard deviation), orientation, phase shift, threshold and quantization steps are set and Gabor filters of two dimension $G^{(s,l)}$ are obtained. The number of filters depends on the value selected for the parameters.

Step 3: Then the convolution of the decompressed image is performed with the obtained Gabor filters and image $U^{(s,l)}$ is obtained after filtering i.e. after convolution.

Step 4: The seven statistical features are taken from all filtered images using equation (6) to equation (13).

Step 5: The feature dimensionality is reduced by merging similar features obtained for different orientations θ in same scale.

Step 6: PCA (Principal Component Analysis) feature selection technique is employed to select and minimize the feature dimension.

Step 7: Classification and analysis of the detection technique with the reduced dimension set is done using random forest classifier.

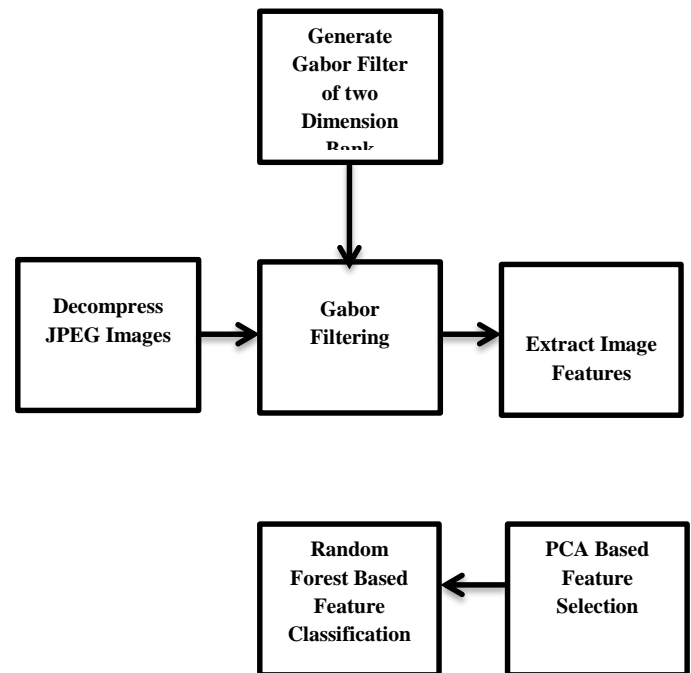


Figure 5. Flow diagram of the presented feature extraction method

RESULTS AND DISCUSSIONS

Here image database and experimental arrangement is discussed. The detection is implemented on the JUNIWARD and nsF5 JPEG steganography. The detection accuracy is compared with present state of art. With PCA the feature dimension is reduced drastically from 10960 to 600. All the codes of steganography and steganalysis are in MATLAB [26]. Finally the result is compared with the other detection method DCT Residuals (DCTR).

Image Database and Experimental Arrangements

In the experiment, 2000 grayscale images of resolution 640 x480 in JPEG format from Greenspun library is used as image database. The quality factor of the image is 95. The stego image is obtained for the capacity 0.05, 0.1 and 0.2 Bit per Non-Zero AC DCT Coefficient (bpac) payloads. For the Gabor filter generation scale is set to 1, threshold value T is set to 4. The value of orientation θ is 32 and phase shift ϕ is set to 0 and $\pi/2$. The random forest had been implemented for data classification and cross-validation. The detection accuracy parameter is obtained for different cases.

Detection Performance of GFB

The dimension of the GFB dimension is 10960 when feature selection is not used. On increasing the number of orientation, the feature dimension also increases. This high value feature dimension makes Gabor based feature very dominant according to the obtained result. But increasing the dimension increases the execution time and memory cost. So, feature reduction is done by implementing. From the table (1), it is

observed that the detection accuracy is almost similar but with very less execution time.

Comparison with Other Methods

The DCT residuals based JPEG steganalysis technique also known as DCTR [22] steganalysis is proposed to be good one. After that the GFR [15] based JPEG steganalysis is introduced

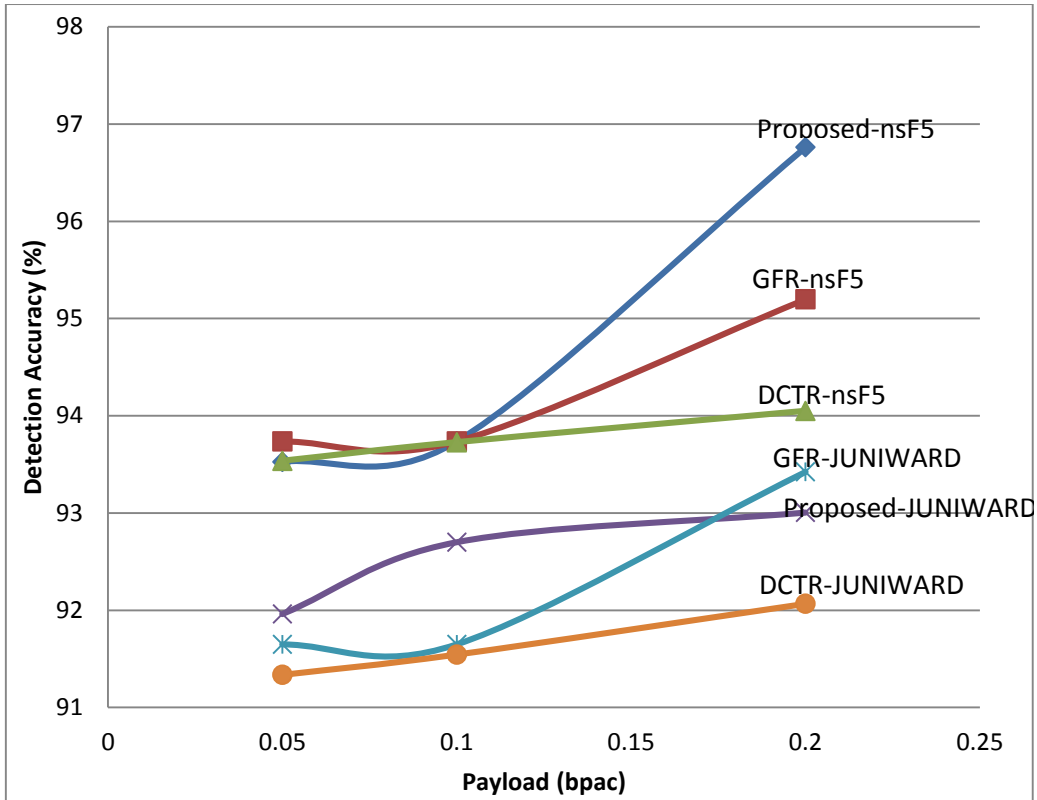
which provides better result than the existing DCTR. In table (2), the performance comparison is done between the proposed technique with the present universal steganalysis techniques i.e GFR and DCTR. From the graph (2) and graph (3), it is observed that the detection accuracy is almost constant with very less execution time.

Table (1) Detection accuracy and execution time of proposed GFB where bpac stands for bit per non zero a.c DCT coefficients

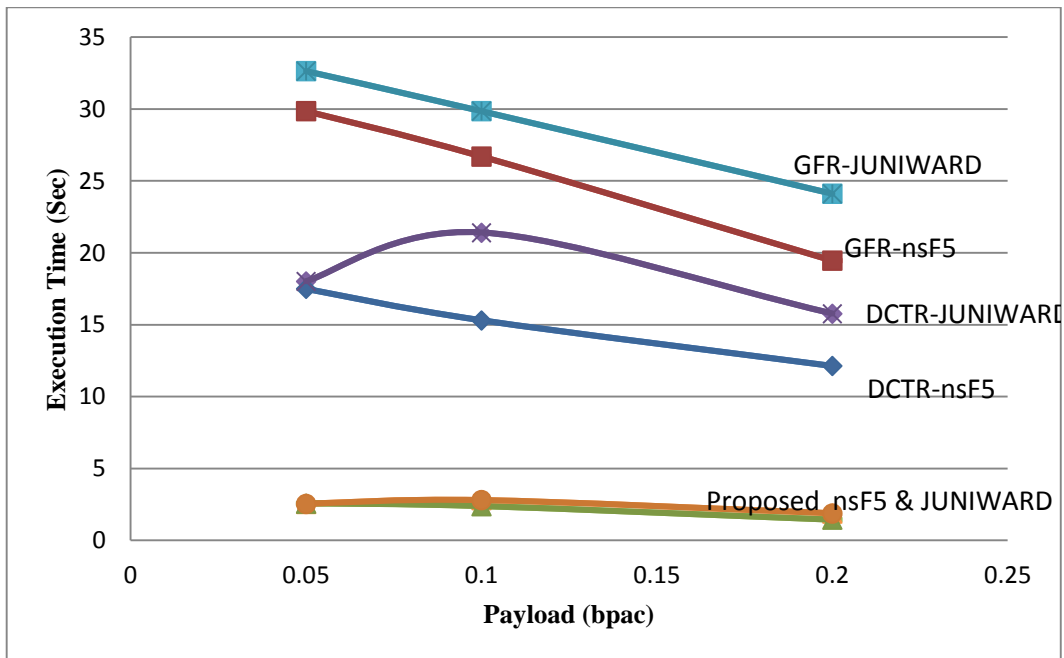
Steganography	Embedding Capacity (bpac)	Sensitivity (TPR)	Precision (PPV)	Specificity (TNR)	AUC	Gini Coefficient	Detection Accuracy (%)
nsF5 [4]	0.05	0.933	0.937	0.937	0.923	0.846	93.528
	0.1	0.937	0.937	0.937	0.955	0.91	93.737
	0.2	0.963	0.973	0.973	0.996	0.992	96.760
J-UNIWARD [10]	0.05	0.920	0.935	0.934	0.92	0.84	91.962
	0.1	0.905	0.937	0.935	0.937	0.874	92.700
	0.2	0.922	0.939	0.938	0.978	0.956	93.006

Table (2) Comparison of the proposed technique with existing JPEG steganalysis techniques

STEGANOGRAPHY	Embedding Capacity (bpac)	Detection Accuracy (%)			Execution Time (Sec)		
		Proposed	GFR [15]	DCTR [22]	Proposed	GFR [15]	DCTR [22]
nsF5 [4]	0.05	93.528	93.737	93.537	2.58	29.85	17.5
	0.1	93.737	93.737	93.7282	2.39	26.7	15.31
	0.2	96.761	95.1983	94.0501	1.45	19.46	12.13
JUNIWARD [10]	0.05	91.962	91.6493	91.3361	2.55	32.63	18.02
	0.1	92.701	91.6493	91.5449	2.81	29.85	21.41
	0.2	93.006	93.4238	92.0668	1.88	24.11	15.77



Graph (1) Representing the detection accuracy for nsF5 and JUNIWARD by proposed GFB, GFR and DCTR for different payload 0.05, 0.1 and 0.2 bpac



Graph (2) Representing the execution time for nsF5 and JUNIWARD by proposed GFB, GFR and DCTR for different payload 0.05, 0.1 and 0.2 bpac

CONCLUSIONS AND DISCUSSION

The proposed work is concerned with the universal steganalysis for the grayscale images. The detection technique highlights the variations in the statistical feature derived from the transformed image.

The analysis parameter of the proposed technique is compared with the recent existing JPEG steganalysis DCTR and conventional GFR technique and it is the finding that efficiency of the proposed technique gives the better results.

The PCA based feature selection and reduction is introduced in the existing GFR based steganalysis technique in which the feature dimension is reduced which reduces the execution time such that the detection accuracy is maintained. The analysis parameter of the proposed technique is compared with the recent existing JPEG steganalysis DCTR and conventional GFR technique and it is the finding that efficiency of the proposed technique gives the better results.

ACKNOWLEDGMENTS

We appreciate Dr. Ayush Singhal who is a Postdoctoral Research Fellow of NCBI (National Institute of Health) in Maryland with his academic profile as PhD, M.Sc from the University of Minnesota, Twin Cities, MN, USA and B.Tech from IIT Roorkee, India for his support in providing the information about WEKA data mining tool and its applications.

REFERENCES

- [1] <http://www.guillermi2.net/stegano/jsteg>.
- [2] <http://www.outgues.org>.
- [3] Westfeld A. F5—A Steganographic Algorithm: High Capacity Despite Better Steganalysis. Proceeding of Fourth International Workshop on Information Hiding. USA, 2001, pp.89-302.
- [4] Fridrich J, Pevný T, and Kodovský J. Statistically Undetectable JPEG Steganography: Dead ends, Challenges, and Opportunities. Proceeding of Second International Workshop on Multimedia & Security, Germany, 2007, pp.3–14.
- [5] Sallee P. Model-Based Steganography. Proceeding of International Workshop on Digital Watermarking, South Korea, 2003, 2939, pp.154-167.
- [6] Song X, Liu F, Luo X, Lu J, and Zhang Y. Steganalysis of perturbed quantization steganography based on the enhanced histogram features. Journal of Multimedia Tools and Applications, December 2015, 74(24), pp.11045–11071.
- [7] Fridrich J, Goljan M, and Soukal D. Perturbed Quantization Steganography. *Journal on Multimedia System*. December 2005, 2(11), pp.98–107.
- [8] Filler T, Fridrich J. Design of Adaptive Steganographic Schemes for Digital Images. Proceeding of International Symposium on Electronic Imaging, Media Watermarking, Security and Forensics of Multimedia, San Francisco, 2011, 7880, pp.1–14.
- [9] Guo L, Ni J, Shi YQ. Uniform Embedding for Efficient JPEG Steganography. *IEEE Transaction in Information Forensic and Security*. May 2014, 9(5), pp.814–825.
- [10] Holub V, Fridrich J. Digital Image Steganography using Universal Distortion. Proceeding of First ACM Workshop on Information Hiding and Multimedia Security, France, 2013, pp.59–68.
- [11] Chhikara R, Prabha Sharma P, Singh L. An Improved Dynamic Discrete Firefly Algorithm for Blind Image Steganalysis. *International Journal of Machine Learning and Cybernetics*. 2016, 7(6), pp.1-15.
- [12] Laimeche L, Farida Merouani H, Mazouzi S. A New Feature Extraction Scheme in Wavelet Transform for Stego Image Classification, *Springer Evolving Systems*. February 2017, pp.1-14.
- [13] Bashkirova D. Convolutional Neural Networks for Image Steganalysis. *Springer Bio Nano Science*. September 2016, 6(3), pp.246–248.
- [14] Karimi H, Shayesteh M, Akhaee A. Steganalysis of JPEG Images using Enhanced Neighbouring Joint Density Features. *IET Image Processing*. July 2015, 9(7), pp.545 –552.
- [15] Song X, Liu F, Yang C, Luo X, Zhang Y. Steganalysis of Adaptive JPEG Steganography using 2D Gabor Filters, Proceeding of 3rd ACM Workshop on Information Hiding and Multimedia Security, USA, 2015, pp.15-23.
- [16] https://en.wikipedia.org/wiki/Gabor_filter.
- [17] Lyu S, Farid H. Detecting Hidden Messages using Higher-Order Statistics and Support Vector Machines. Proceeding of International Workshop on Information Hiding, Netherlands, 2003, 2578, pp.340–354.
- [18] Fridrich J. Feature-Based Steganalysis for JPEG Images and its Implication for Future Design of Steganographic Scheme. Proceeding of International Workshop on Information Hiding, Canada, 2005, pp.67–81.
- [19] Chen B, Feng G, Zhang X, Li F. Mixing High-Dimensional Features for JPEG Steganalysis with Ensemble Classifier, *Springer Signal, Image and Video Processing* 2014, 8(8), pp.1475–1482.

- [20] Pevny T, Fridrich J. Merging Markov and DCT features for Multiclass JPEG Steganalysis. *Steganography and watermarking of Multimedia Contents*. February 2007, 6505, pp.1–13.
- [21] Kodovsky J, Fridrich J. Steganalysis of JPEG Images using Rich Models. *SPIE, Electronic Imaging, Media Watermarking, Security and Forensics*. February 2012, 8303, pp.23–25.
- [22] Holub V, Fridrich J. Low Complexity Features for JPEG Steganalysis using Undecimated DCT. *IEEE Transactions on Information Forensics and Security*, October 2014, 10(2), pp.219 - 228.
- [23] Holub V, Fridrich J. Phase-Aware Projection Model for Steganalysis of JPEG Images. *SPIE Media Watermarking, Security and Forensics*, March 2015, 9409, pp.8–12.
- [24] Song X, Liu F, Zhang Z, Yang C, Luo X, Chen L. 2D Gabor Filters-Based Steganalysis of Content-Adaptive JPEG Steganography, *Springer Multimedia Tools and Applications*. December 2016, pp.1-29.
- [25] Gul G, Kurugollu F. JPEG Image Steganalysis using Multivariate PDF Estimates with MRF Cliques. *IEEE Transactions on Information Forensics and Security*. March 2013, 8(3), pp.578 - 587.
- [26] <http://dde.binghamton.edu/download.edu/download/syndrome>.
- [27] https://en.wikipedia.org/wiki/Principal_component_analysis.
- [28] Denemark T, Boroumand M, Fridrich J. Steganalysis Features for Content Adaptive _____ JPEG Steganography. *IEEE Transactions on Information Forensics and Security*, April 2016, 11(8), pp.1736-1746.
- [29] Mohammadi FG, Abadeh MS. Image Steganalysis using a Bee Colony Based Feature Selection Algorithm. *Elsevier Engineering Applications of Artificial Intelligence*, May 2014, 31, pp.35-43.
- [30] Pathak P, Selvakumar S. Blind Image Steganalysis of JPEG images using Feature Extraction through the Process of Dilation, *Elsevier Digital Investigation*, March 2014, 11(1), pp. 67-77.